

UC Irvine

UC Irvine Previously Published Works

Title

Axicon-based annular laser trap for studies on sperm activity

Permalink

<https://escholarship.org/uc/item/9q747115>

Authors

Shao, Bing
Vinson, Jaclyn M
Botvinick, Elliot L
[et al.](#)

Publication Date

2005-08-18

DOI

10.1117/12.613116

Copyright Information

This work is made available under the terms of a Creative Commons Attribution License, available at <https://creativecommons.org/licenses/by/4.0/>

Peer reviewed

Axicon-based annular laser trap for studies on sperm activity

Bing Shao^{*a}, Jaclyn M. Vinson^a, Elliot L. Botvinick^b, Sadik C. Esener^a, Michael W. Berns^b

^aDept. of Electrical and Computer Engineering, Univ. of California/San Diego, 9500 Gilman Dr.,
La Jolla, CA 92093-0409

^bDept. of Bioengineering, Univ. of California/San Diego, 9500 Gilman Dr., La Jolla, CA 92093-
0412

ABSTRACT

As a powerful and noninvasive tool, laser trapping has been widely applied for the confinement and physiological study of biological cells and organelles. Researchers have used the single spot laser trap to hold individual sperm and quantitatively evaluated the motile force generated by a sperm. Early studies revealed the relationship between sperm motility and swimming behavior and helped the investigations in medical aspects of sperm activity. As sperm chemotaxis draws more and more interest in fertilization research, the studies on sperm-egg communication may help to explain male or female infertility and provide exciting new approaches to contraception. However, single spot laser trapping can only be used to investigate an individual target, which has limits in efficiency and throughput. To study the chemotactic response of sperm to eggs and to characterize sperm motility, an annular laser trap with a diameter of several hundred microns is designed, simulated with ray tracing tool, and implemented. An axicon transforms the wavefront such that the laser beam is incident on the microscope objective from all directions while filling the back aperture completely for high efficiency trapping. A trapping experiment with microspheres is carried out to evaluate the system performance. The power requirement for annular sperm trapping is determined experimentally and compared with theoretical calculations. With a chemo-attractant located in the center and sperm approaching from all directions, the annular laser trapping could serve as a speed bump for sperm so that motility characterization and fertility sorting can be performed efficiently.

Keywords: Optical trapping, Sperm motility, Chemotaxis, Axicon, Annular trap, Fertilization.

1. INTRODUCTION

With the deterioration of the environment and an increasing economic interest on animal husbandry, artificial insemination has become indispensable. It has enormous benefit to various animal farms including fish farms, as well as zoological societies that attempt to save endangered species. To make artificial insemination more effective, fertility experts grade sperm according to their overall quality before freezing them for future use. Among many factors involved in the expression used to quantify sperm quality grading, initial motility score (IMS) (i.e., the product of initial motility (MOT%) and the square of speed of progression (SOP) score¹), and hyperactivity (i.e., a distinctive motility pattern of sperm characterized by vigorous flagellar movements essential for fertilization²), play the two most dominant roles. Noninvasive and high efficiency analysis of sperm motility and hyperactivity is of great significance for artificial insemination and genetic improvement programs. Most traditional techniques evaluate the sperm qualitatively on a one by one base, which is labor intensive, and can only offer subjective results that depend on the observer. These considerations give rise to a strong need for an automated, quantitative, and objective assessment tool for sperm quality. In the last decade, computer aided sperm analysis (CASA) has been developed to offer objective assessment of sperm motility for large population. However, the thin chambers (30 μ m) used in CASA impact the behavior of sperm swimming with large transverse amplitude (e.g. monkey sperm)³, and the errors encountered by CASA when dealing with phase contrast images often misinterprets actual sperm count in the field. Finally, while CASA can measure the motility of sperm, the force information potential useful in sperm viability assessment is lost.

*bshao@soliton.ucsd.edu; phone: 1 858 822-4158; fax: 1 858 524-1225

Optical Trapping and Optical Micromanipulation II, edited by Kishan Dholakia, Gabriel C. Spalding
Proceedings of SPIE Vol. 5930 (SPIE, Bellingham, WA, 2005) · 0277-786X/05/\$15 · doi: 10.1117/12.613116

Laser trapping, especially in the near infrared regime, as a noninvasive and microfluidic-compatible biomedical tool, has been widely applied for the confinement and physiological study of biological cells^{4,5} and organelles⁶. Since the late 1980s, researchers have been using single spot laser tweezers to trap individual sperm and quantitatively evaluate the motile force generated by a sperm while it is swimming^{7,8}. With the help of laser tweezers, the relationship between sperm motility and swimming pattern was revealed⁷ and the effects of medical aspects of sperm activity were investigated^{9,10}.

Although single spot laser trapping provides a quantitative analysis of individual sperm motility, it has several drawbacks. For example, an untrapped sperm may interact with the trapped sperm invalidating the measurement (Fig. 1). When a sperm of interest was caught by the laser tweezers and held for a time sufficient enough for motility analysis (Fig. 1 (a-b)), a second sperm swam through the trapping spot interfering with the analysis of the initially trapped sperm (Fig. 1 (c-d)). Additionally, serial individual sperm analysis using a single point laser trap makes large-quantity evaluation time consuming, and lacks the ability of in-situ sorting based on motility and hyperactivity. Finally, as the study of sperm chemotaxis in sperm-egg interactions becomes increasingly of interest in fertility research, the application of laser trapping may have application in the study of the sperm's response to a diffusion gradient of an attractant¹¹. The use of single spot laser traps applied to individual sperm would be limiting as opposed to an approach that would allow for parallel analysis of a large number of sperm.

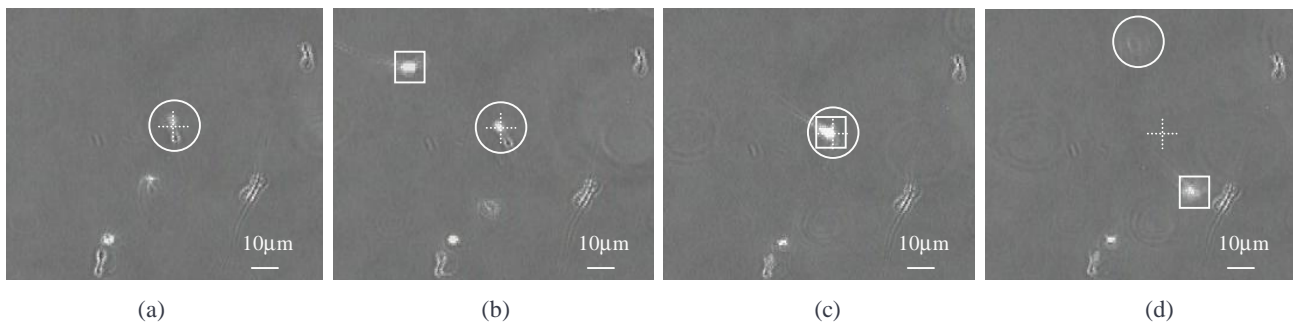


Figure 1: Interference to sperm analysis with single spot trapping introduced by non-targeted sperm. (a). A sperm (inside the white circle) is trapped by a single spot laser trap (indicated by the white dotted cross hair) for analysis. (b). A second sperm (inside the white square) swims towards the trapping spot. (c). The second sperm swims into the trapping spot, and disturbs the analysis of the first trapped sperm. (d). Both sperm swim out of the trap.

This study demonstrates the use of a ring-shaped laser trap, which can not only serve as a force shield to protect the analytical field from other sperm (Fig. 2 (a)), but could enable parallel sorting and separation of sperm as a function of their motility and chemotaxis response (Fig. 2 (b-c)). The advantage of a “ring trap” over a “single point trap” or “line trap” lies in its ability to provide an equal-distance (from the center) condition, which is important for a biological tropism study in which chemical stimuli may diffuse radially from a point source. When an attractant is fixed in the center of the ring, laser power can be adjusted so that only sperm swimming with sufficient energy and sensitivity to the attractant's local concentration gradient will have enough energy to pass through the trap and reach the attractant. We expect this new method of optical trapping will bring high efficiency and high throughput (measurements on many sperm at the same time) measurements to a vast variety of bio-tropism (phototaxis, geotaxis, galvanotaxis, etc.) studies.

There are several different ways to create an annular trap. Mechanical scanning can form a ring with a fast scanning focus spot. However, this will reduce the average exposure time and introduce a tangential drag force that might affect the sperm. More importantly, the scanning speed of present mechanical scanners is not high enough to work with fast moving targets such as sperm swimming with speeds up to 200µm/s. Diffractive optics and holography can also be used to create ring shape traps but generally have lower efficiency. The efficiency of optics is an important consideration in sperm trapping since a single sperm trap requires 100~200mW at the specimen plane. Although a computer generated hologram (CGH) can introduce flexible changes of the ring size and trapping depths, it requires a high resolution spatial light modulator. An axicon, also known as a conical lens or rotational symmetrical prism, on the other hand, has low cost, negligible energy loss, and high flexibility. Considering these advantages, the annular laser trap was built with axicon lenses.

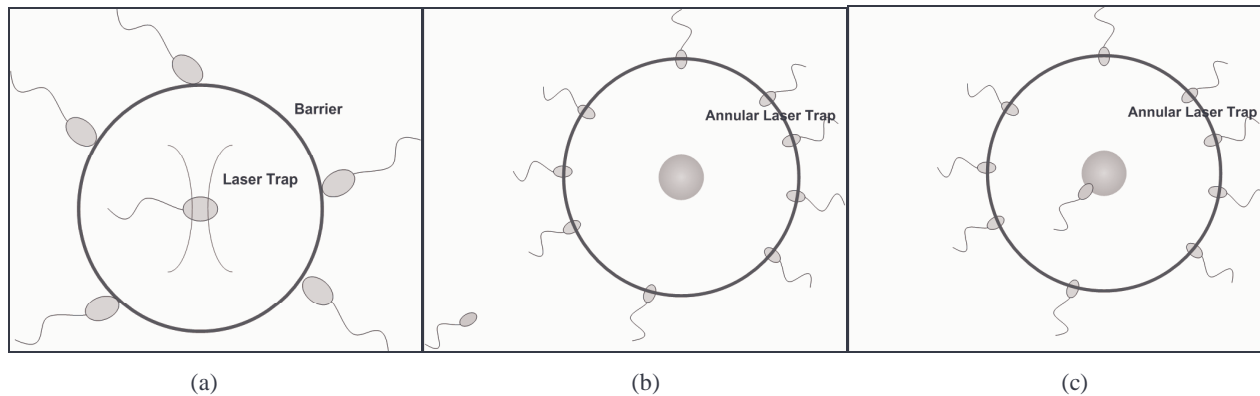


Figure 2: Applying a ring-shaped laser trap to facilitate sperm quality analysis. (a). A ring trap works as a force shield to protect sperm held by single point laser trap from interference introduced by other untrapped sperm. (b). In sperm motility and chemotaxis research, weak sperm with low swimming power and response to central attractant are held back by the optical gradient field of the ring trap. (c). A sperm with strong response to the central attractant develops an above-threshold swimming force to pass the ring trap and reach the attractant in the center of the ring.

2. DESIGN OF OPTICAL SYSTEM

Earlier research⁵ has shown that the deviation of a trapping spot from the optical axis δ is nearly linearly proportional to the inclination angle θ of the input beam. Uniform annular trapping requires that incident light be composed of collimated beams from all directions ($0\sim 360^\circ$ azimuthal angle) with the same tilting angle θ to the optical axis, in other words, the input light must be a cone of collimated beam intersecting at the back aperture of objective. To obtain a high enough gradient force for confinement, the back aperture of the objective should be completely filled, i.e. the thickness of the cone should be equal to the diameter of the back aperture.

Accordingly, an optical system was designed using an axicon. As a lens composed of a flat surface and a conical surface, an axicon has the unique ability to bend normally incident light toward its tip without affecting its divergence angle (degree of collimation). The bending angle is determined by the parameters of the axicon, therefore, by selecting different base angles or materials (index of refraction) of the axicon, output light cones with different apex angles can be obtained. As shown in Fig. 3, the input laser beam is collimated, expanded by a telescope lens pair and directed normally to the flat surface of an axicon. The beam emerging from the conical surface of the axicon is bent toward the optical axis at an angle $\beta = \arcsin(n \sin \gamma) - \gamma$, where γ is the base angle of the axicon and n is the refractive index of the lens material. A focusing lens converges the cone of collimated beams into a ring on the conjugated image plane of the specimen plane. This ring is then imaged in the specimen plane via the tube lens-objective combination.

Since the focusing lens and the tube lens are working together as a telescope, the inclination angle θ of the light beams input into the objective can be simply expressed as

$$\theta = \frac{f_{FL}}{f_{TL}} \beta \quad (1)$$

where f_{FL} and f_{TL} are the focal lengths of the focusing lens and the tube lens, respectively.

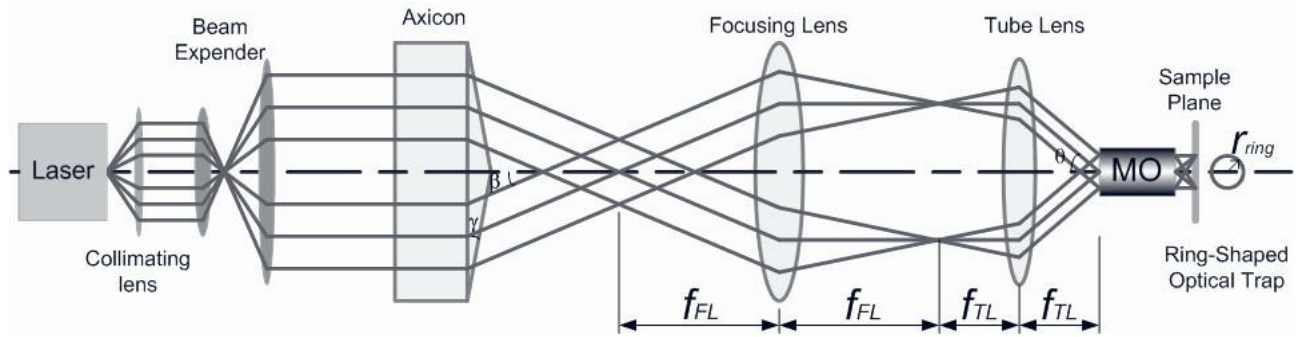


Figure 3: Schematic diagram of the optics designed for annular laser trapping (not to scale), MO---Microscope Objective.

Accordingly, the radius of the ring trap can be calculated as

$$r_{ring} = \delta = f_{EFL} \cdot \tan(\theta) = f_{EFL} \cdot \tan\left(\frac{f_{FL}}{f_{TL}} \beta\right) = f_{EFL} \cdot \tan\left[\frac{f_{FL}}{f_{TL}} (\arcsin(n \sin \gamma) - \gamma)\right] \quad (2)$$

where f_{EFL} is the effective focal length of the microscope objective.

3. SIMULATIONS

3.1 System parameters

The wavelength we used for trapping was 1064 nm. To obtain as high power throughput as possible, the laser beam was directed to the objective through the epi-fluorescence port (arc lamp path) of an inverted microscope (Axiovert 200M, Zeiss, Germany) with the arc lamp tube system removed. In this way, the microscope-embedded tube lens that is anti-reflection (AR) coated for visible light was avoided, and a 1064 nm AR-coated plan-convex singlet lens ($f_{TL}=400\text{mm}$, KPX208AR.18, Newport, Irvine, CA) was used as a substitute. A 1" BK7 ($n=1.506$) axicon lens with broad-band AR coating and base angle $\gamma=10^\circ$ (Del Mar Photonics, San Diego, CA) was chosen so that together with the focusing lens ($f_{FL}=100\text{mm}$, KPX187AR.18, Newport, Irvine, CA), the tube lens and the microscope objective (EC Plan-Neofluar, DIC, 40 \times NA=1.3, oil immersion, Zeiss, Germany), a ring trap with a diameter of hundreds of micrometers could be formed.

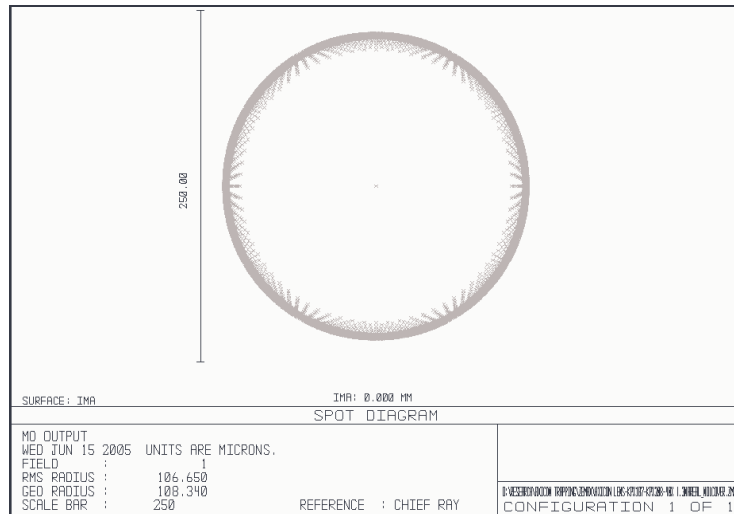
3.2 Ray tracing simulation

Ray tracing simulations with ZEMAX (Bellevue, WA) were conducted with a plane wave input using the parameters listed in section 3.1. As shown in Fig. 4 (b) - (d), a sharp and clear ring focus is formed on the specimen plane in the simulation. Although some rays fail to focus due to the off-axis aberration coma, both the spot diagram (Fig. 4 (b)) and the cross-section (Fig. 4 (c)) show that they only occupy a negligible percentage. From the Huygens PSF cross-section in transverse plane Fig. 4 (d), two intensity peaks with high gradient can be clearly seen, which indicate a strong gradient force on the specimen plane.

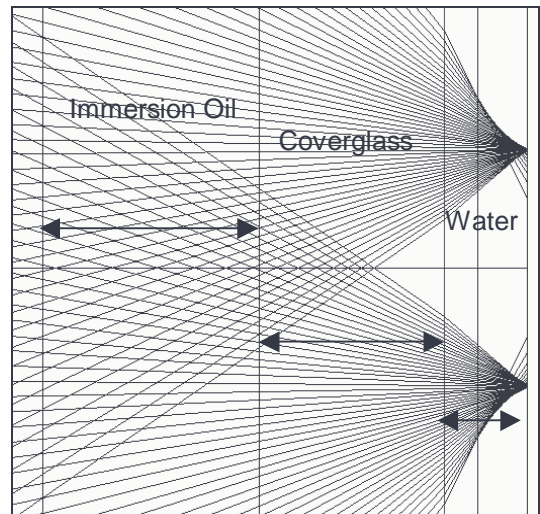
The radius of the ring obtained from the spot diagram simulation (Fig. 4 (b)) is about 210 μm , which agrees well with the calculation accordingly to Eqn. (2) that predicts 200 μm .



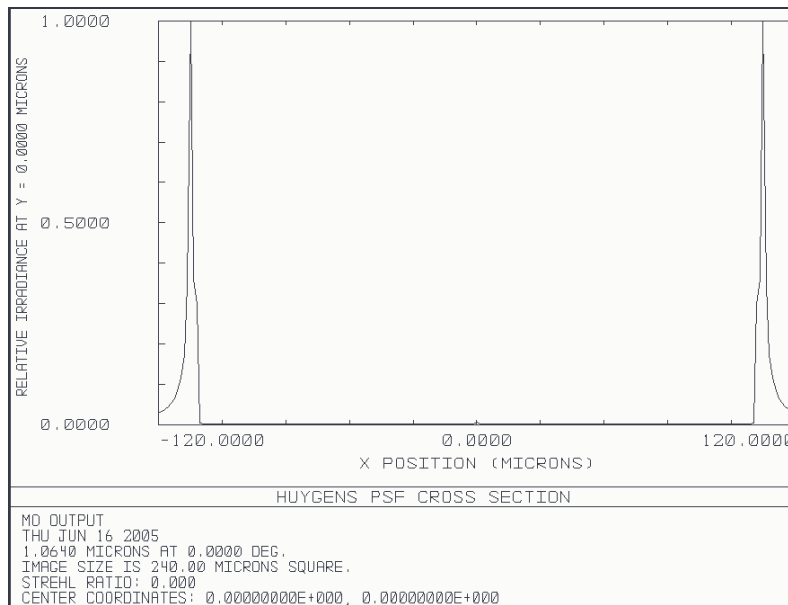
(a)



(b)



(c)



(d)

Figure 4: ZEMAX simulations of axicon-based ring trap system. (a). System layout. (b). Spot diagram at the specimen plane shows the size and quality of the ring focus. (c). Close-up of the system layout near the specimen plane gives a cross-section view of the ring focus formation, only negligible amount of rays failed to focus due to coma. (d). Huygens PSF cross-section shows a strong gradient of light intensity on the specimen plane.

4. EXPERIMENTS

4.1 Experimental setup

The scheme of the system used in our experiments is shown in Fig. 5. The light beam from a fiber laser with 1064 nm wavelength (YLD-5-LP, IPG Photonics, Oxford, MA) is directed to a beam splitter and 50% of it is used for the annular trap (the other 50% is used for a steerable single point trap, which could be combined with the annular trap to enhance the system performance in the future). The telescope lens 1 and telescope lens 2 collimate and expand the beam to a desired size so that the back aperture of the objective is completely filled. Mirror 1 and Mirror 2 are directing the light to the axicon, where the collimated input beam is divided with respect to the optical axis and bent towards it at an angle $\beta=5.16^\circ$. The back focal plane of the axicon, the focusing lens, the tube lens and the back aperture of the microscope objective are forming a 4- f system, therefore the input to the objective is a light cone composed of collimated light from all the azimuthal angles with a thickness equal to the diameter of the back aperture. A second 4- f system is composed of the ring image at the back focal plane of the focusing lens, the tube lens, the objective, and the specimen plane.

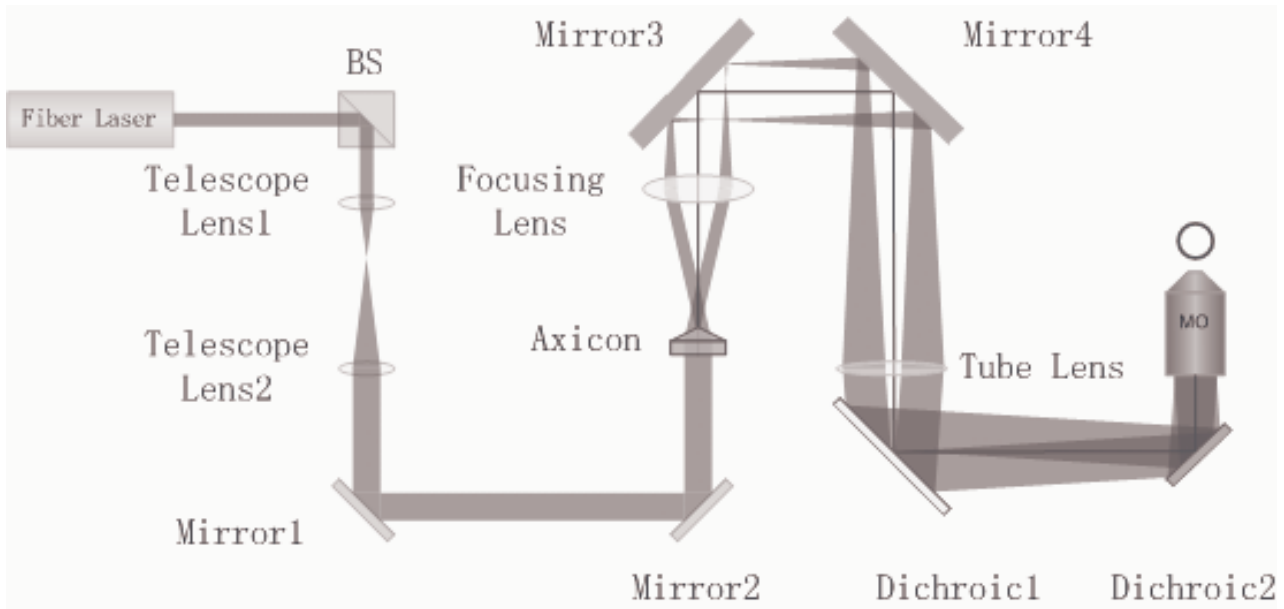


Figure 5: Experimental setup of the annular laser trap. BS---Beam Splitter; MO---Microscope Objective.

4.2 Experiments with microspheres

Experiments with 15 μm diameter polystyrene microspheres (2015A, Duke Scientific, Palo Alto, CA) were carried out to demonstrate the feasibility of the ring-shaped trap. A microsphere-water suspension was put into a plastic dish with a 0.017 mm thick glass cover-slip as the bottom (P35G-1.5-14-C, MatTek, Ashland, MA). With a post-objective power of 80mW, microspheres were attracted into the field of view and a full ring of microspheres was created along the fine annular focus (Fig. 6). The diameter of the ring was about 210 μm , which agreed well with the calculation and simulation results. The average trapping power was estimated to be 2.4mW/microsphere, assuming a uniform distribution of power along the ring. The bright pattern in the center was due to the scattering and internal reflection of the microscope optics at the glass/water interface and stray light. From Fig. 6 (a) to Fig. 6(b), it can be seen that leftward stage translation collected additional microspheres (initially on the right side of the ring) into the annular focus, forcing subsequent redistribution of the “squeezed” microspheres within the ring. The beads originally confined in that part of the ring focus were pushed circumferentially within the circle (as shown with the black arrows), indicating a strong optical gradient field in the radius direction, and no confinement effect circumferentially. This observation agrees with Fig. 4 and the principle of trapping.

To calibrate the gradient force of the ring trap, the microscope stage was translated laterally. According to Stokes’ law,

$$f_{grad} = f_{drag} = 6\pi\eta av \quad (3)$$

where f_{grad} increases as the microsphere displace radially from the ring, and is maximal at a flow rate at which the trap can barely hold the microsphere. With an estimated averaged trapping power of 2mW/microsphere, and using the viscosity of water as $\eta=1\times 10^{-3}$ Nsm⁻², it was determined that the critical flow rate occurs when the stage is translated with a speed of 7 μ m/s, corresponding to a gradient force of 1pN.

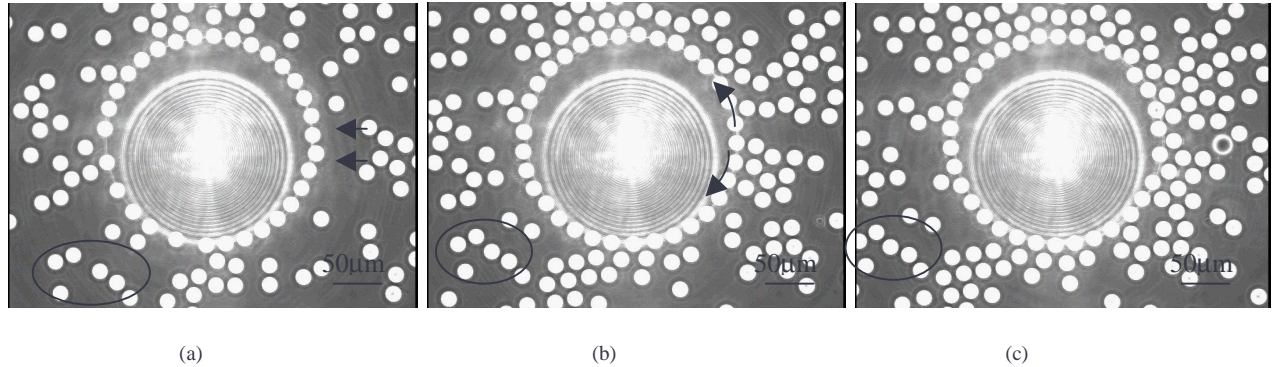


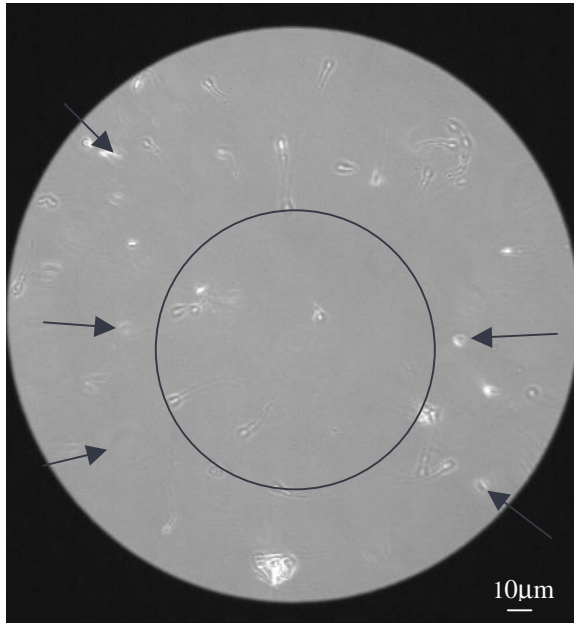
Figure 6: Video frames of annular laser trapping of 15 micron polystyrene spheres in water with 40 \times NA1.30 oil immersion objective. (a). With the stage at the original position, a ring of microspheres was formed along the annular focus of the laser beam. (b). Frame taken after translating the stage to the left with a speed of 1 μ m/s for 10 seconds. (c). Frame taken after a subsequent leftwards translation of the stage with speed of 2 μ m/s for 10 seconds. The 6 beads in the white ellipse were used as a reference.

4.3 Experiment with sperm

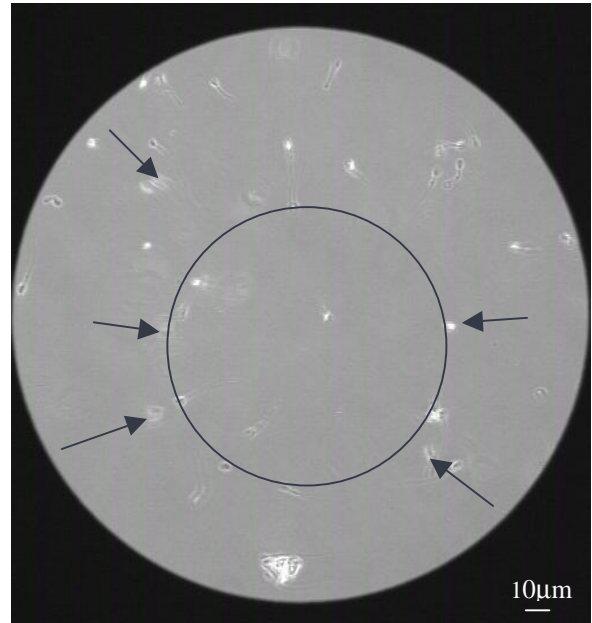
Dog sperm (provided by the Conservation and Research for Endangered Species (CRES), Zoological Society of San Diego, CA) were used. The sperm were stored in liquid N₂ (-196 $^{\circ}$ C, 77K) until needed for experimentation^{12,13}. The sperm were first thawed in a pre-warmed water bath (37 $^{\circ}$ C) for approximately 30 to 60 seconds. Sperm were then transferred to an Eppendorf tube and centrifuged at 2000 rpm for 10 minutes. Excess waste was removed and the sperm pellet was re-suspended in 1mL of pre-warmed BWB (Biggers–Whitten–Whittingham)+ BSA (Bovine serum albumin) media (1mg of BSA per 1mL of BWB, osmolality of 270 – 300 mmol/kg water, pH of 7.2 – 7.4)¹⁴. Final dilutions were created from this stock solution (desired final concentration of 106,000 sperm per milliliter of BWB).

Since dog sperm generally swim at a velocity of 20~200 μ m/s¹⁵, at least 50mW is required for each sperm to be trapped or slowed down. Accordingly, with a ring diameter of 210 μ m, which can hold about 100 sperms, a minimum post-objective total power of 5W is needed. Considering a 2/3 loss through the microscope objective, this corresponds to a pre-objective power of about 15W. Since the current setup can only supply at most 30mW/sperm on the specimen plane (with a 10W input power from the laser), the sperm were barely affected except for some observed scattering effects. With a higher output laser, or smaller ring-size, a power of 100mW/sperm should be easily achieved, and the desired trapping effects observed.

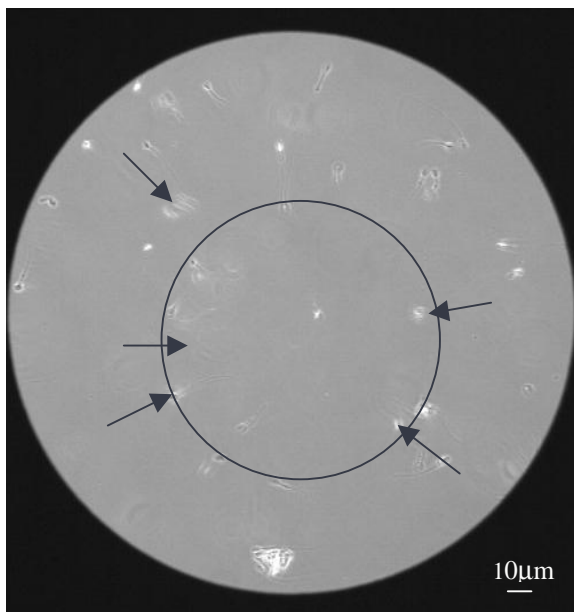
Fig. 7 shows a preliminary result of dog sperm exposed to approximately 30mW/sperm. Sperm with low to medium swimming speeds were attracted and then scattered out of the focal plane as soon as they encountered the ring-focus, which means that the ring-shaped laser trap does affect the sperm. However, the weak gradient force was not strong enough to trap most of the sperm. Further improvement approaches will be brought up in the Discussion section.



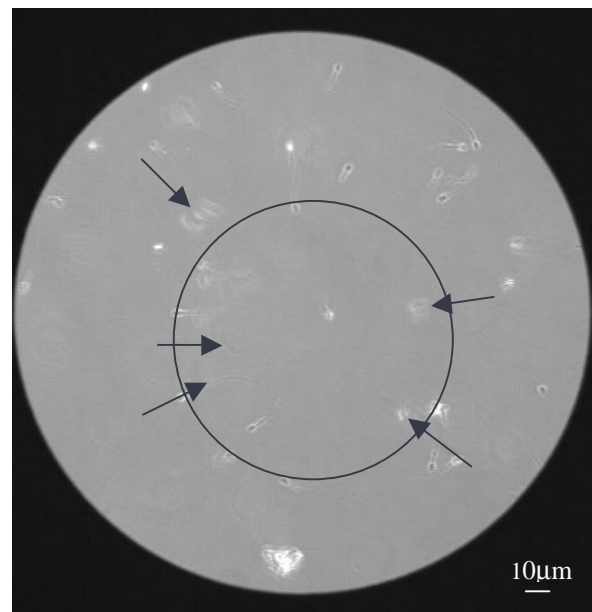
(a)



(b)



(c)



(d)

Figure 7: Video frames from experiment with dog sperm show a ring-shaped reaction zone where the sperm got attracted and scattered. (a). Frame #190; (b). Frame #220; (c). Frame # 245; (d). Frame #253.

5. DISCUSSION

5.1 Optimization of the trapping performance

As mentioned in the last section, the gradient force obtained with the current system is not enough to trap high motility sperm. In addition to the power limitation, there are two factors that affect the trapping performance.

First, since the axicon divides all the incoming beams with respect to the optical axis and bends them towards its apex angle, the light emerging from it will enter the objective lens from every direction (all azimuthal angles). In ZEMAX simulation, a plane wave with uniform intensity was used, therefore, after the axicon, all the beams incident to the objective for trapping still have uniform intensity patterns. However, when a Gaussian input is used in a practical system, an asymmetrical intensity pattern (half-Gaussian) beam from each azimuthal angle will result (Fig. 8). According to Fourier transformation, this input beam with an asymmetrical intensity distribution leads to a tilted phase front at the specimen plane, which indicates that the total photon momentum transfer is not perpendicular to the specimen plane, and the stability of the trap is significantly degraded. By modifying the input beam profile to a top-hat, the asymmetrical intensity distribution after the axicon can be eliminated, and the stability of the trap can be improved.

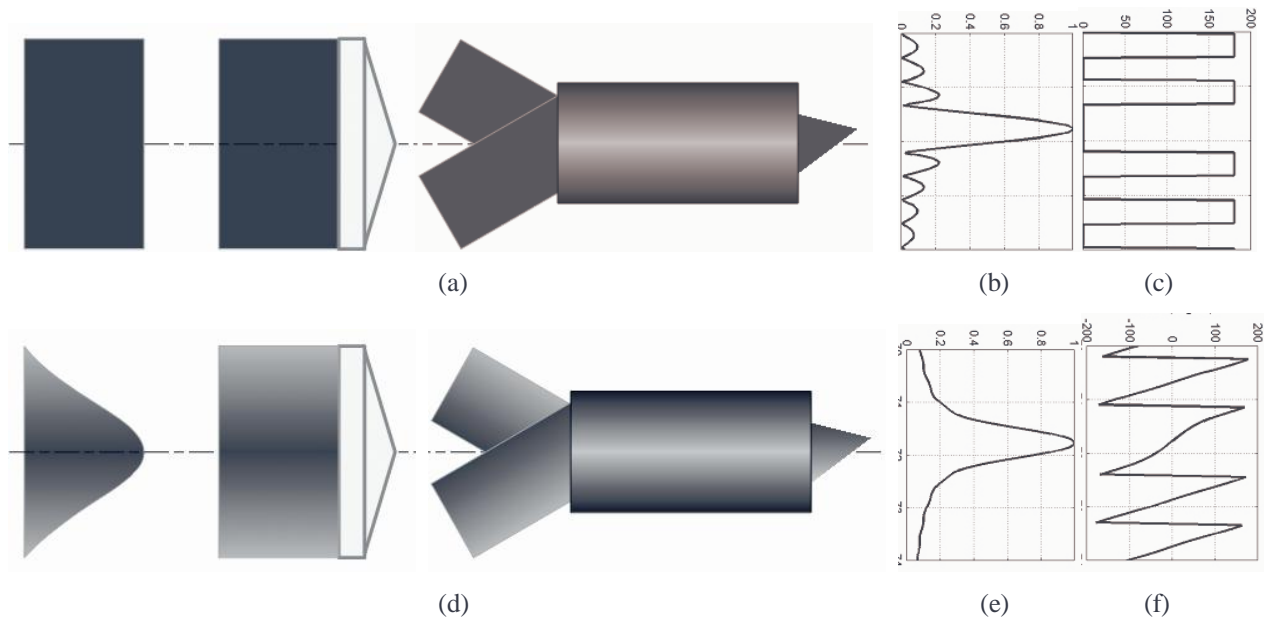


Figure 8: Effect of input beam intensity distribution on trapping performance of the ring. (a). For a plane wave incident with uniform intensity, each beam emerging from the axicon in one azimuthal angle incident the objective lens with a uniform intensity. (b). The intensity distribution on the back focal plane of the objective (specimen plane). (c). The phase distribution on the specimen plane after the objective is symmetrical. (d). For a Gaussian input, whose intensity decreases from the center, the beams after the axicon have a non-uniform and non-symmetrical intensity patterns. (e). The intensity distribution on the specimen plane after the objective. (f). The phase distribution on the specimen plane after the objective is not symmetrical.

The second factor that affects the performance of the annular trap is the tilting of the sample holder with respect to the ring focus. This leads to a flow of the particles in the specimen plane and makes one part of the ring trap stronger than the other. This undesired effect could be compensated for via adjusting the tilting of the sample holder.

5.2 Dynamically-adjustable annular laser trap

With fixed total power, changing the size of the annular trap leads to a change of the trapping power per spot. This could be used for quantitative evaluation and sorting of sperm with different swimming forces, motility patterns, and chemotaxis responses to the egg and other chemo-attractants.

By introducing two additional axicons between the focusing lens and the tube lens, and translating one of the axicons along the optical axis, the apex angle of the incident light cone is changed, which results in a diameter change of the ring-shaped trap¹⁶.

The trapping depth could also be varied by introducing a lens pair⁵ in front of the first axicon.

6. CONCLUSIONS

An optical system for an annular laser trapping based on an axicon lens was designed. Simulation results show a sharp and clear ring-shaped focus on the specimen plane, whose diameter agrees well with both the theoretical calculation and the experimental measurement. The high gradient of intensity indicates a strong trapping force. Experiments with microspheres demonstrated the feasibility of the ring-trap and its ability to generate gradient forces in the radial direction that are strong enough to trap microspheres under low laser power (~2mW/sphere) and to shift particles along the ring due to the zero gradient forces in circumferential direction. Preliminary experiments on actively swimming dog sperm showed a ring-shaped reaction zone. Further optimization of the system is needed in order to generate a gradient force strong enough to slow down or trap fast swimming sperm.

With these results, we believe the ring trap can serve as a parallel and quantitative analytical tool for fertility and biotropy research.

ACKNOWLEDGEMENTS

The authors thank Scripps Institute of Oceanography for financial supporting, Dr. Barbara Durrant of the Zoological Society of San Diego, Beckman center for Conservation and Research for Endangered Species (CRES) for the dog sperm.

REFERENCES

1. B. Durrant, D. Amodeo, A. Anderson and M. Ann Olson, "Effect of extraction methods on cryopreservation of canine epididymal sperm", *SSR 33rd Annual Meeting*, July 15-18, 2000, Madison, WI, USA, **BAR-4-5-3**.
2. H. Schmidt and G. Kamp, "Induced hyperactivity in boar spermatozoa and its evaluation by computer-assisted sperm analysis", *Reproduction*, **128**, pp171-179, 2004.
3. J. Baumber and S. A. Meyers, "Hyperactivated Motility in Rhesus Macaque (*Macaca mulatta*) Spermatozoa", submitted to *J. Andrology*.
4. M. Ozkan, M. M. Wang, C. Ozkan, R. A. Flynn and S. Esener, "Optical manipulation of objects and biological cells in microfluidic devices", *Biomedical Microdevices*, **5**, pp47-54, 2003.
5. B. Shao, S. Zlatanovic, S. C. Esener, "Microscope-integrated micromanipulation based on multiple VCSEL traps", *Optical Trapping and Optical Manipulation*, edited by Kishan Dholakia, Gabriel C. Spalding, *Proc. SPIE*, **5514**, pp62-72, 2004.
6. M. W. Berns, "Laser scissors and tweezers", *Scientific American (International Edition)* **278**, pp52-57, 1998.
7. Y. Tadir, W. H. Wright, O. Vafa, T. Ord, R. H. Asch, M. W. Berns, "Micromanipulation of sperm by laser generated optical trap", *Fertil. Steril.* **52**, pp870-873, 1989.
8. Y. Tadir, W. H. Wright, O. Vafa, T. Ord, R. H. Asch, M. W. Berns, "Force generated by human sperm correlated to velocity and determined using a laser generated optical trap", *Fertil. Steril.* **53**, pp944-947, 1990.
9. P. Patrizio, Y. Liu, G. J. Sonek, M. W. Berns, and Y. Tadir, "Effect of pentoxifylline on the intrinsic swimming forces of human sperm assessed by optical tweezers", *J. Andrology* **21**, pp753-756, 2000.
10. Z. N. Dantas, E. Araujo, Jr., Y. Tadir, M. W. Berns, M. J. Schell, S. C. Stone, "Effect of freezing on the relative escape force of sperm as measured by a laser optical trap", *Fertil. Steril.* **63**, pp185-188, 1995.
11. M. Eisenbach, and I. Tur-Kaspa, "Do human eggs attract spermatozoa?", *BioEssays*, **21**, pp203-210, 1999.
12. Harper, S.A., B.S. Durrant, K.D. Russ and D. Bolamba, "Cryopreservation of domestic dog epididymal sperm: A model for the preservation of genetic diversity", *J. Andrology*, **19** (Suppl), pp50, 1998.
13. Durrant, B., S. Harper, D. Amodeo, A. Anderson, "Effects of freeze rate on cryosurvival of domestic dog epididymal sperm", *J. Andrology*, **21**(Suppl), pp59, 2000.
14. Biggers JD, W.W., Whittingham DG. "The culture of mouse embryos in vitro", *Methods of mammalian embryology*, Freeman, San Francisco, pp86-116, 1971.

15. J. M. Vinson, E. L. Botvinick, B. Durrant, M. W. Berns, "Correlation of sperm' swimming force as assessed by optical tweezers to their swimming speed", in press.
16. B. Shao, J. M. Vinson, E. L. Botvinick, D. Song, S. Zlatanovic, S. C. Esener, M. W. Berns, "Dynamically adjustable annular laser trapping for sperm chemotaxis study", *OSA Topical meetings 2005, Information Photonics*, June 5-9, Charlotte, NC, USA, ITuC4.